

State of Health and Charge Estimation Based on Adaptive Boosting integrated with particle swarm optimization/support vector machine (AdaBoost-PSO-SVM) Model for Lithium-ion Batteries

Ran Li¹, Wenrui Li^{2,*}, Haonian Zhang²

¹ Engineering Research Center, Ministry of Education of Automotive Electronics Drive Control and System Integration, Harbin University of Science & Technology, Harbin, China

² School of Electrical and Electronic Engineering, Harbin University of Science & Technology, Harbin, China

*E-mail: dapangjing@163.com

Received: 3 October 2021 / Accepted: 20 November 2021 / Published: 5 January 2022

The state of charge (SOC) and state of health (SOH) of a power battery system are the research hotspots of researchers in recent years. An accurate state estimation is conducive to research on battery life optimization and guarantees the safe driving of electric vehicles. The use of artificial intelligence, machine learning and other methods has always been the mainstream of research on SOC and SOH prediction, but there are defects such as a strong data dependence, a large calculation volume and a long-time consumption. In view of this, a battery SOC-SOH online estimation method is proposed in the previous work of this paper based on PSO-SVM algorithm to solve the above problems. However, due to the PSO-SVM algorithm, there is a problem that the stability of the estimated battery SOH is not high. Therefore, an integrated learning AdaBoost algorithm is introduced in this paper to improve the PSO-SVM regression model, meanwhile through integrated processing, multiple weak learners are combined to construct a strong regression. Simulation and experimental analysis show that this method has a good data adaptability and accuracy, whose average estimation error does not exceed 2.316.

Keywords: Lithium battery, SOH, AdaBoost, SVM, BMS

1. INTRODUCTION

With the continuous development of society and economy, energy shortages and environmental pollution have gradually become issues of concern to all countries in the world. Lithium-ion batteries are the main power source of electric vehicles with their advantages including a low self-discharge, a high energy density and no environmental pollution.[1] However, the performance of such batteries is

constantly changing over time. Among them, the state of health of the battery (SOH) is an important parameter of the battery management system. An online SOH estimation can ensure the safety of electric vehicles. Increasing the penetration rate of electric vehicles has far-reaching significance.

There are many factors influencing the SOH, and common estimation methods mainly include experimental measurement method, model building method and data-driven method. Experimental measurement methods are divided into direct experimental methods and indirect analysis methods. Direct experimental methods mainly include volumetric test method [2] and internal resistance test method [3], and indirect analysis methods are mainly based on volumetric incremental analysis method (ICA) [4] and ultrasonic method [5]. The test accuracy of experimental measurement methods is high, but it is limited by the experimental environment, which is not conducive to practical engineering applications; the model establishment method is mainly used to establish an equivalent circuit model of batteries, and the corresponding battery experiments are conducted to identify the relevant parameters of circuits, so as to realize the estimation of the battery SOH. Common model building methods mainly include the equivalent circuit model [6-8] (ECM) and the electrochemical model [9-11] (EM), whose advantage is that they can well reflect the internal working status of a battery, but the disadvantage is that the relevant model parameters need to be constantly updated. Inaccurate model parameters will lead to larger errors in the prediction of battery SOH; the data-driven method [12-16] is more like a black box, battery users do not need to understand the internal operating mechanism of a battery, extract relevant battery health characteristics or make reasonable predictions about the health of the battery through relevant machine learning and intelligent optimization algorithms. Researchers have shown that commonly used battery aging characteristics include capacity, internal resistance [17-19], battery cycle times [20], stacking pressure [21] and SEI impedance [22], etc. Common data-driven methods include SVM model, neural network model and Gaussian process regression (GPR) model. Nuhic et al. [13] proposed a GPR model to predict the SOH, but it takes a certain amount of time to reasonably adjust the parameters in its parameter settings; Bai et al. [14] proposed a lithium-ion battery SOH estimation model based on the integration of artificial neural network and double extended Kalman filter algorithm, but the artificial neural network method consumes a long time and is easily overfitted. Klass et al. [12] built a model of SVM and virtual machine to estimate battery SOH. By collecting battery current, voltage, SOC and temperature, the battery temperature can be well estimated. There is a good non-linear regression model for support vector machine algorithm (SVM), so it is widely used by scholars to estimate the health of a battery.

A PSO-SVM-based online research method is proposed in the literature [23] for the health state of lithium-ion batteries, through which relevant aging characteristics are extracted and a PSO-SVM-based method is used to predict the SOH of a battery. The innovation of this method lies in the innovative proposal of a new coupling relationship between SOC and SOH. Compared with the traditional complex fitting coupling relationship, this coupling relationship does not require too many adaptability conditions to make the SOC and SOH of a battery able to be closely integrated; the online estimation of battery SOH is realized, which solves the problem that the traditional SOH estimation involves a large amount of calculation and can only be estimated offline. However, this method has a deficiency of a low estimation accuracy. Since the particle swarm algorithm has disadvantages including a low accuracy and easy divergence in the early stage of the algorithm, when the algorithm converges to a certain accuracy,

the optimization cannot be continued, making the achievable accuracy low and causing serious consequences to actual production and life.

Therefore, in order to solve the problem that the PSO-SVM algorithm is not stable when estimating the battery SOH, a method is proposed in this paper based on the AdaBoost-PSO-SVM algorithm to predict the battery SOH. The PSO-SVM algorithm and the APSO-SVM algorithm are used in turn to test the test data for 50 times, and the errors of the 50 prediction results of the APSO-SVM algorithm are compared with those of the PSO-SVM algorithm. Simulation analysis shows that the AdaBoost-integrated PSO-SVM algorithm has a better estimation stability and accuracy than the PSO-SVM algorithm; secondly, the algorithm is analyzed for adaptability, and the simulation analysis shows that the AdaBoost-integrated PSO-SVM is used. The algorithm has a good adaptability. Finally, compare the estimation error results of other papers to prove the effectiveness of the algorithm.

The differences between this article and the previous work lie in the following points:

(1) Keep some necessary mathematical models (PSO-SVM, feature extraction model), and add an introduction to the AdaBoost model.

(2) The relationship between battery SOC and discharge voltage in the process of battery aging is supplemented; a more vivid drawing method is used to draw the relationship between battery SOC and time as well as that among SOH, discharge voltage, time and SOC. It can be seen from the figure that with the continuous aging of a battery, the color of the corresponding characteristic quantity changes from light to dark, which can enable readers to better understand the new coupling relationship between battery SOC and SOH.

(3) The parameter settings of the algorithm are appropriately adjusted in this article. Since the previous work is focused on the coupling relationship between SOH and SOC, the estimation of SOC will not be discussed in this article, which, while, will focus on how to improve the estimation stability of SOH.

(4) In view of some problems in the previous work, the AdaBoost model is used to integrate the PSO-SVM regression model and to improve the stability as well as accuracy of the prediction.

2. ALGORITHM PRINCIPLE

2.1. Principle of PSO-SVM

The VC dimension theory and the structure minimization theory are combined in the SVM algorithm. By constructing an optimal hyperplane in the sample space, the distance between the hyperplane and different sample sets is maximized, so as to obtain the best promotion ability. Through the establishment of input and output mapping models, the regression prediction of battery SOH is realized. In this paper, the radial basis kernel function continues to be used as the basis function. The mathematical formula of the radial basis function is shown in Formula (1):

$$K(x_i, x_j) = \exp\left(-\frac{\|x_i - x_j\|^2}{2\delta^2}\right) \quad (1)$$

In Formula (1), δ is the kernel parameter of the algorithm, and the difference of $x_i - x_j$ is the input variable of the radial basis kernel function of the algorithm.

A SVM algorithm has two important parameters, namely the penalty parameter and the kernel parameter. Grid search is used to find suitable parameters in traditional SVM algorithms, which is not suitable for too large parameter search ranges. When the parameter search range becomes larger, scholars use corresponding optimization algorithms to improve the search ability. Particle swarm algorithm has simple principles and a strong practicability, which is widely used to optimize SVM algorithms.

The particle swarm algorithm mainly imitates the behavior of group cooperation when birds are foraging. Each potential solution is regarded as a particle, which updates itself by following two extreme values, namely individual extreme value and global extreme value, through which the optimal solution is found. Figure 1 shows the flow chart of particle swarm optimization support vector machine:

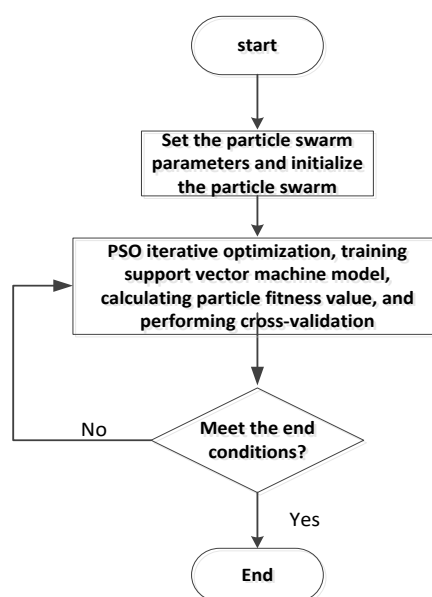


Figure 1. PSO-SVM algorithm

2.3. Principle of AdaBoost

The Adaptive Boosting (AdaBoost) algorithm is an adaptive enhanced integration algorithm in a boosting integration algorithm proposed by Freund and Schapire et al. [24] in 1997, which is an adaptive enhanced integration algorithm. A classical boosting algorithm has two shortcomings. The first is that the sample weight cannot be adjusted so that weak learners can learn more pertinently. The second is that multiple weak learners cannot be integrated into a stronger learner through a boosting algorithm. It has made corresponding improvements to the deficiencies of boosting algorithms in these two aspects, whose core idea is to train the weak regression with different prediction accuracies for the same set of training data for many times, and then fuse multiple weak regressions to form a strong regression with a higher accuracy. In essence, this algorithm is realized by changing the distribution of data. According to the calculation results of each weak regression, its weight is adaptively adjusted. For the samples with large errors in the weak regression, the weight of each sample is increased. New data updated by weight

is input to the later training weak regression for training, and finally the weak and dry weak regressions are merged.

The algorithm flow of AdaBoost strong regression is as follows:

The training set are $T = \{(x_1, y_1), (x_2, y_2), \dots, (x_N, y_N)\}$, where N is the logarithm of the training set. $x_i \in R^n$, $y_i \in R$, $i = 1, 2, \dots, N$.

1) Initialize the weight distribution of training samples, the initial weights of each training sample are equal:

$$w_{1i} = \frac{1}{N} \quad (2)$$

$$D_1 = (w_{11}, w_{12}, \dots, w_{1N}) \quad (3)$$

2) The training samples with sample weight D_m ($m = 1, 2, \dots, M$) are used for training. The current iteration number is denoted as m, and the weak regression $G_m(x)$ is obtained. The training error of each training sample in the weak regression is :

$$e_{i,m} = |G_m(x_i) - y_i| \quad (4)$$

The prediction error rate of $G_m(x)$ on the training dataset is:

$$E_m = P(e_{i,m}, \theta) = \sum_{i=1}^N w_{m,i} I(e_{i,m} > \theta) \quad (5)$$

Where θ is the predefined threshold.

3) According to the calculated regression error rate E_m , determine the weight coefficient α_m of the mth regressor $G_m(x)$ in the final strong regressor. The expression is as follows:

$$\alpha_m = \frac{1}{2e^{E_m}} \quad (6)$$

4) After each iteration, the weight is updated according to the sample error, the expression of the $w_{m+1,i}, D_{m+1}$ is as follows:

$$w_{m+1,i} = \begin{cases} \frac{w_{m,i}}{Z_m} \times 1.1, & e_i(t) > \theta \\ \frac{w_{m,i}}{Z_m}, & e_i(t) \leq \theta \end{cases} \quad (7)$$

$$D_{m+1} = (w_{m+1,1}, w_{m+1,2}, \dots, w_{m+1,i}, \dots, w_{m+1,N}) \quad (8)$$

Where Z_m is the normalization factor, it is used to ensure that the total weight is 1, the calculation method is as follows:

$$Z_m = \sum_{i=1}^N w_{m,i} \quad (9)$$

Finally, all weak regressors are integrated into a strong regressor as shown in the formula:

$$G(x) = \sum_{m=1}^M \alpha_m G_m(x) \quad (10)$$

A single learner can be used to accurately predict the health status of a battery, which, however, will have a certain probability of error results. Once an error prediction occurs, it will have a bad impact on the whole battery system. Therefore, when multiple learners are used, the probability of an error

prediction can be assigned to different learners according to a certain weight, so as to realize risk diversification and improve the stability of the whole prediction model [25-28].

2.4. Advantages of AdaBoost

Although a single learner can also be used to accurately predict the health of a battery, there is a certain probability that it will lead to wrong results. Once a wrong prediction occurs, it will definitely have a bad impact on the entire battery system. Therefore, when multiple learners are used, the probability of an incorrect prediction can be assigned to different learners according to a certain weight, thereby realizing risk diversification and improving the accuracy as well as stability of the entire prediction model.

3. LI-ION BATTERY CAPACITY DEGRADATION DATA

Public battery data provided by NASA is mainly used as simulation experiment data in this article. The battery numbers used in this study are B0005, B0018 and B0007, which are named battery #1, battery #2 and battery #3, whose battery model is lithium iron phosphate battery. The nominal capacity is 2Ah, and batteries #1, #2 and #3 are running in three working states, namely charging, discharging and measuring internal resistance. All the three working conditions are in the same room-temperature (24°C) environment. First of all, a battery is charged with a constant current of 1.5A until the voltage reaches 4.2V, which is then charged with a constant voltage until the current drops below 20mA. During the discharge phase, the battery is discharged with a constant current of 2A until the voltage reaches 4.2V, which is the corresponding discharge cut-off voltage. Table 1 shows the relevant working conditions of the battery.

Table 1. Battery charging and discharging working status

Battery Number	Charge Cutoff Voltage (V)	Discharge Cutoff Voltage (V)	Charging Current (A)	Discharge Current (A)	Rated Capacity (Ah)
#1	4.2	2.7	1.5	2	2
#2	4.2	2.5	1.5	2	2
#3	4.2	2.2	1.5	2	2

Battery #1 is used as training data to test battery #2 and battery #3 respectively in this article. The following Figure 2 shows the SOH diagram of the batteries. When the capacity decays to 70% of the rated capacity, a battery is considered to be invalid [30], it can be seen from Figure 3 that battery #1 covers the working environment of batteries as much as possible, so it can be used as training data to test battery #2 and battery #3. At the same time, the capacity decline of battery #2 was faster than that

of battery #1, while that of battery #3 is slower than that of battery #1, and that of battery #3 has not fallen to the failure threshold. Therefore, when predicting battery #3, the corresponding estimation error will be higher than the predicted error of battery #2.

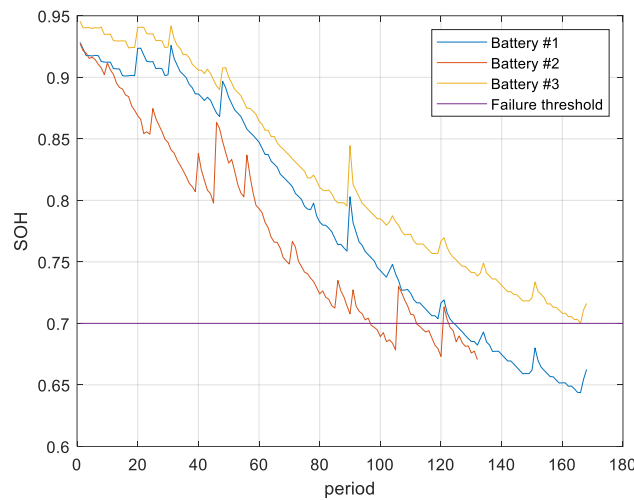


Figure 2. Battery capacity degradation

4. MODEL ESTABLISHMENT

4.1. Algorithm parameter setting

Compared with the previous work, the search range of the penalty parameter is adjusted in this article, which is changed to (0.1,100), meanwhile the search range of the kernel parameter is adjusted and changed to (0.001,1000), set the number of weak learners as 5, and the settings of other parameters are the same as the previous working settings [31]. The purpose of adjusting the parameter search range is to speed up the search and improve the prediction accuracy.

4.2. Definition of SOH

There are many ways to define SOH [29], here we use capacity to define SOH, and the defined expression is as follows:

$$\text{SOH} = \frac{Q_{\max}}{Q_n} \times 100\% \quad (11)$$

Among them, Q_{\max} is the current maximum usable capacity of the battery, and Q_n is the normal capacity of the battery

4.3. Model building

The SOH of batteries is in a slowly changing state. With battery aging, the capacity of batteries declines more and more. At the meantime, the curve among SOC, discharge voltage and discharge time

also gradually changes. Figure 3 shows the relationship between SOC and time. The colors in the figure represent the attenuation of the batteries, the rightmost black color is the first discharge for them, the green color in the middle is the 84th discharge of them, and the manganese purple on the far left is the 168th discharge of them. With battery decaying, the overall color of battery SOH also changes from light blue to dark blue, and it can be seen from Figure 3 that with battery decaying, the slope of SOC is also increasing with the discharge time.

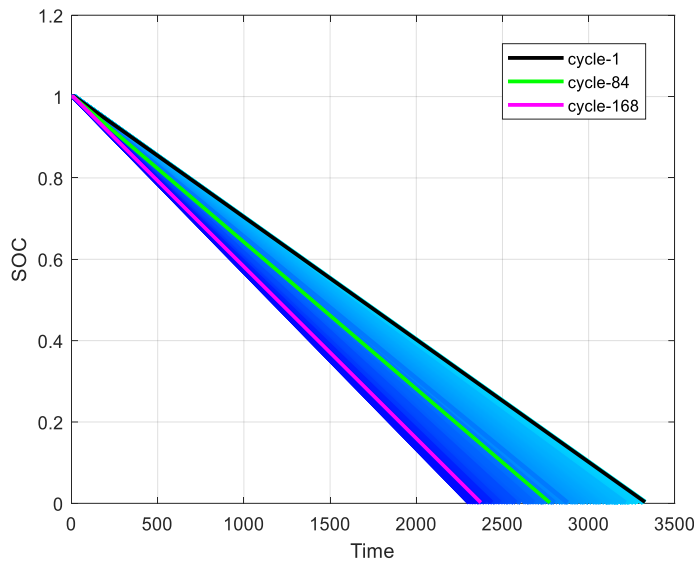
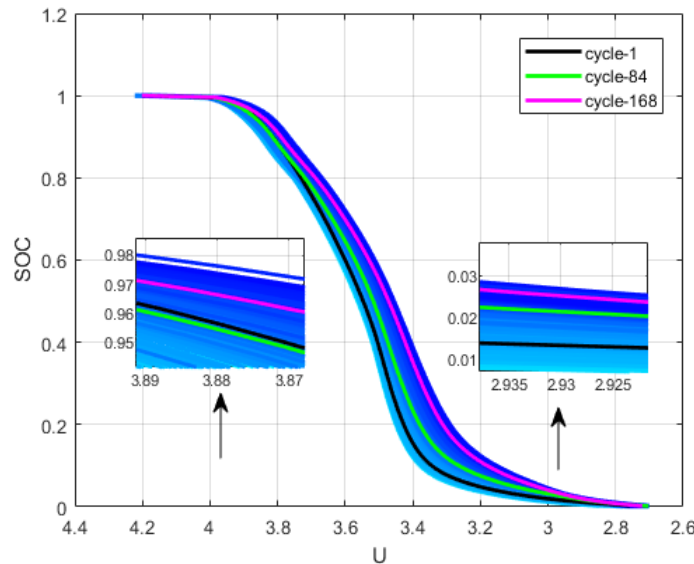
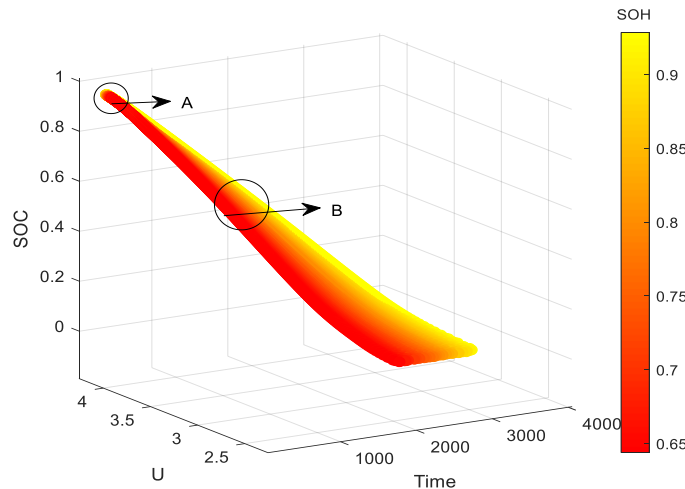


Figure 3. SOC-Time relationship

Figure 4 shows the relationship between SOC and discharge voltage of battery #1. The black color on the far right is the first discharge of the batteries, the green color in the middle is the 84th discharge of them, and the manganese purple on the far left is the 168th discharge of them. After discharge, with battery aging, the overall color of the batteries also changes from light blue to dark blue. It can be seen from Figure 4 that while SOH of a battery changes, the slope of SOC and the discharge voltage gradually decreases, which shows that with battery aging, the discharge voltage of batteries also accelerates. In Figure 4, the graphs of SOC and voltage in the voltage range (3.89-3.87) (2.935-2.925) are enlarged respectively. It can be found from the figure that in the voltage range (3.89-3.87), the first and the 84th discharge curve are closely connected, but the 168th discharge curve is very different from these two discharge curves, which shows that the batteries have experienced an obvious aging. In the voltage range (2.935-2.925), the first discharge curve drops smoothly, but the 168th discharge curve drops quickly, which can also indicate that the batteries are in the 168th discharge, in which obvious aging phenomenon has appeared.

**Figure 4.** SOC-U relationship

It can be seen from the above that factors affecting battery aging include battery SOC, discharge time and discharge voltage. A set of determined SOC, discharge time and discharge voltage can correspond to a unique SOH. The new coupling relationship between SOC and SOH is shown in Figure 5.

**Figure 5.** New coupling diagram of SOC and SOH

It can be found from Figure 5 that SOH of the battery is gradually decreasing. As the color changes from yellow to dark red, it represents the deepening of battery aging. A total of 168 discharge curves are drawn in the figure, each of which represents different battery SOH states, which are represented by the color bar on the right side of the figure, therefore, the predictive expression of SOH is as follows:

$$SOH = f(SOC, T, U) \quad (12)$$

However, a lot of calculation pressure will be brought to the computer if SOH of the batteries is predicted directly through the above method, and the corresponding storage space is also very limited. Therefore, a new type of SOC-SOH coupling relationship is adopted to simplify the calculation complexity. When determining the value of Z-axis SOC, it will correspond to a two-dimensional coordinate (Time, U), the value of which corresponding to the same SOC value is also different, as is shown in the figure. Select the 168th curve as an example to illustrate the extraction of aging feature quantity, and select (U, Time) corresponding to Point A and Point B as the aging feature quantity, the above two can determine the battery health curve of the 168th discharge. With this feature, the battery SOH can be predicted based on the AdaBoost-PSO-SVM (APSO-SVM), and the estimation expression is as follows:

$$SOH = f(T_{soc=100\%}, U_{soc=100\%}, T_{soc=current\%}, U_{soc=current\%}) \quad (13)$$

4.4. Evaluation criteria

The mean relative error (MRE) and the root mean square error (RMSE) are used as criteria for judging the accuracy of the algorithm:

$$MRE(\%) = \frac{1}{N} \sum_{i=1}^N \left| \frac{y_i - \hat{y}_i}{y_i} \right| \times 100\% \quad (14)$$

$$RMSE = \sqrt{\frac{1}{N} \sum_{i=1}^N (y_i - \hat{y}_i)^2} \quad (15)$$

Among them, N refers to the number of sample data, y_i represents the true value of SOH, and \hat{y}_i represents the predicted value of SOH

5. SOH PREDICTION

5.1. Simulation analysis

Battery #1 is used as training data, and battery #2 is used as test data. Since these batteries are actually tested under laboratory conditions, 9 representative SOC discharge intervals are selected in this paper, each of which can make a prediction of the batteries' state of health. The nine discharge intervals are shown in Figure 6. The subsequent discharge interval sequence of Figure 7, 8, 9, 10 and 11 is also the same as that of Figure 6. For simplicity and beauty, each discharge interval will not be marked in the subsequent figures in detail. The PSO-SVM algorithm and the APSO-SVM algorithm are used in turn to test the test data 50 times, and the errors of the 50 prediction results of the APSO-SVM algorithm as well as the PSO-SVM algorithm are compared. The comparison result is shown in Figure 6:

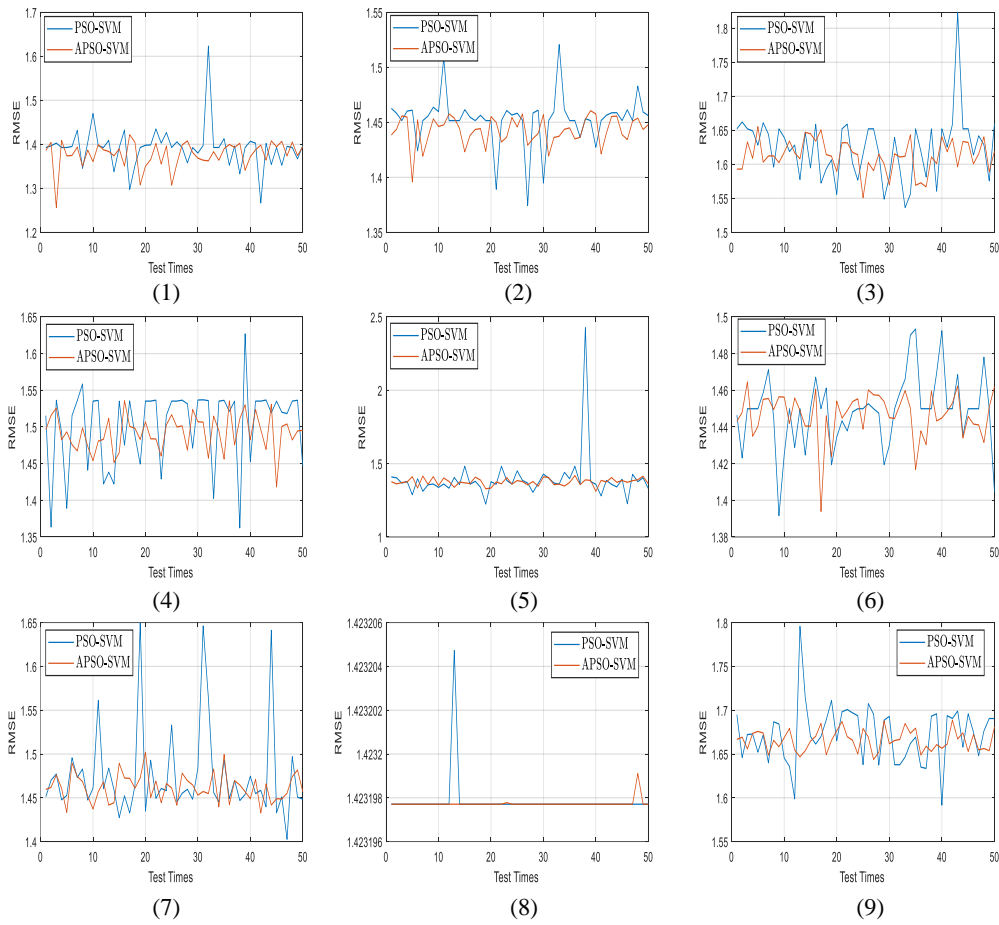


Figure 6. RMSE comparison of battery #2 (1) SOC interval(100%-10%) ,(2) SOC interval(100%-20%), (3) SOC interval(100%-30%) , (4) SOC interval(100%-40%) , (5) SOC interval(100%-50%) , (6) SOC interval(100%-60%) , (7) SOC interval(100%-70%) , (8) SOC interval(100%-80%) , (9) SOC interval(100%-90%)

As is shown in Figure 6, when PSO-SVM is used to estimate the battery SOH, there will be several abnormal prediction results in each discharge interval of a battery. A more typical one is that when the SOC discharge interval is within the interval of 100%-50% and PSO-SVM is used in the 38th prediction, the RMSE is 2.427, far exceeding the average error of 1.4. On the contrary, the overall estimation result through APSO-SVM algorithm is relatively stable, which is lower than the average estimation result of PSO-SVM. Comparing the 9 SOC discharge intervals in the figure, it is not difficult to find that the prediction result and stability based on APSO-SVM are better. Select the value of the abnormal time as the prediction result of PSO-SVM, and compare it with the prediction result of APSO-SVM. SOH prediction of battery #2 is shown in Figure 7.

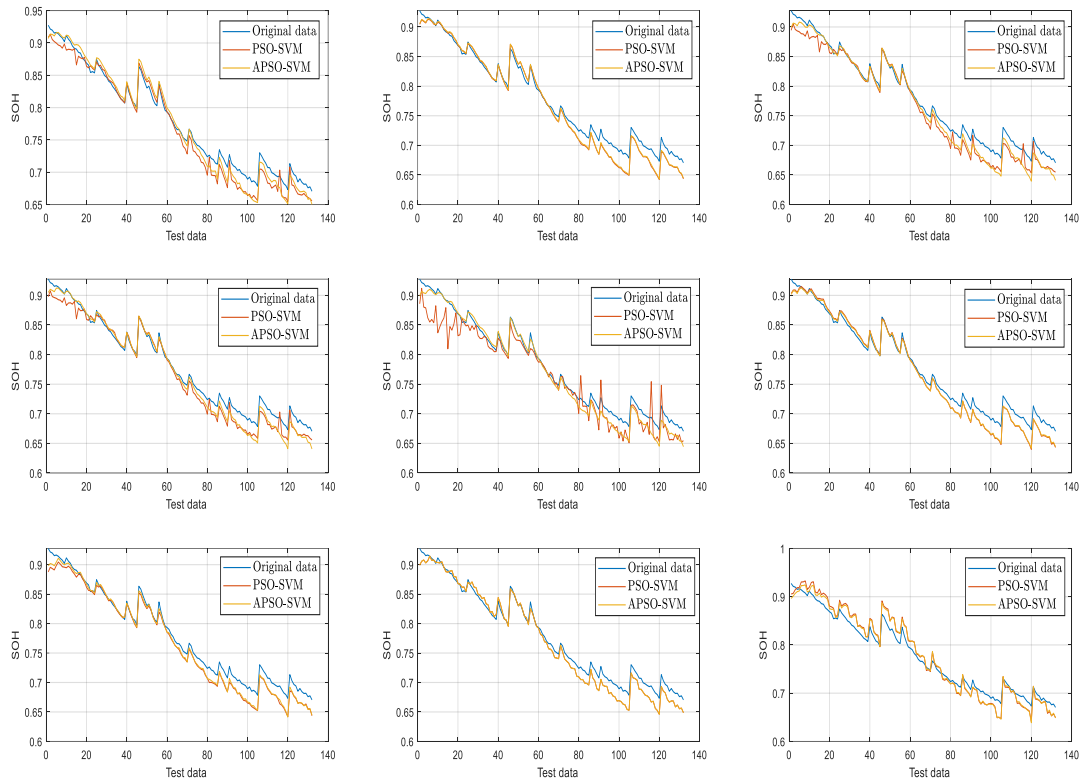


Figure 7. SOH prediction for battery #2

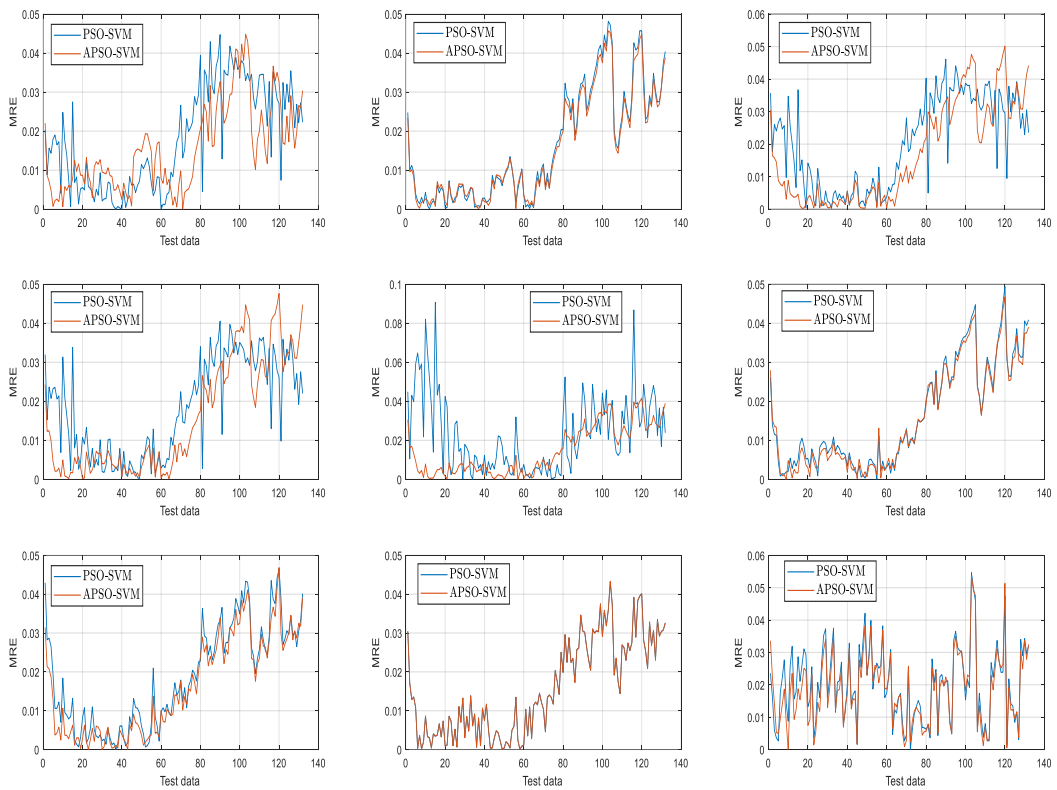


Figure 8. Comparison of mean relative error

As is shown in Figure 7, the estimation effect of multi-learner (APSO-SVM) is stronger than that of single-learner (PSO-SVM), and the prediction curve of APSO-SVM is also closer to the true health state of the batteries, which avoids the probability of large errors in PSO-SVM and improves the stability of a health estimate of battery state. The estimation effect of the two algorithms is compared in Figure 8 from the perspective of mean relative error (MRE), and the conclusions obtained are the same as before.

5.2. Adaptability analysis of the algorithm

The discharge cut-off voltage of battery #2 is 2.5V, and that of battery #3 is 2.2V. There are some differences in the working status of the two batteries, which can be used for adaptive analysis. Therefore, the selection of training data remains unchanged, the test data is changed to battery #3, and the estimated effect is shown in Figure 9:

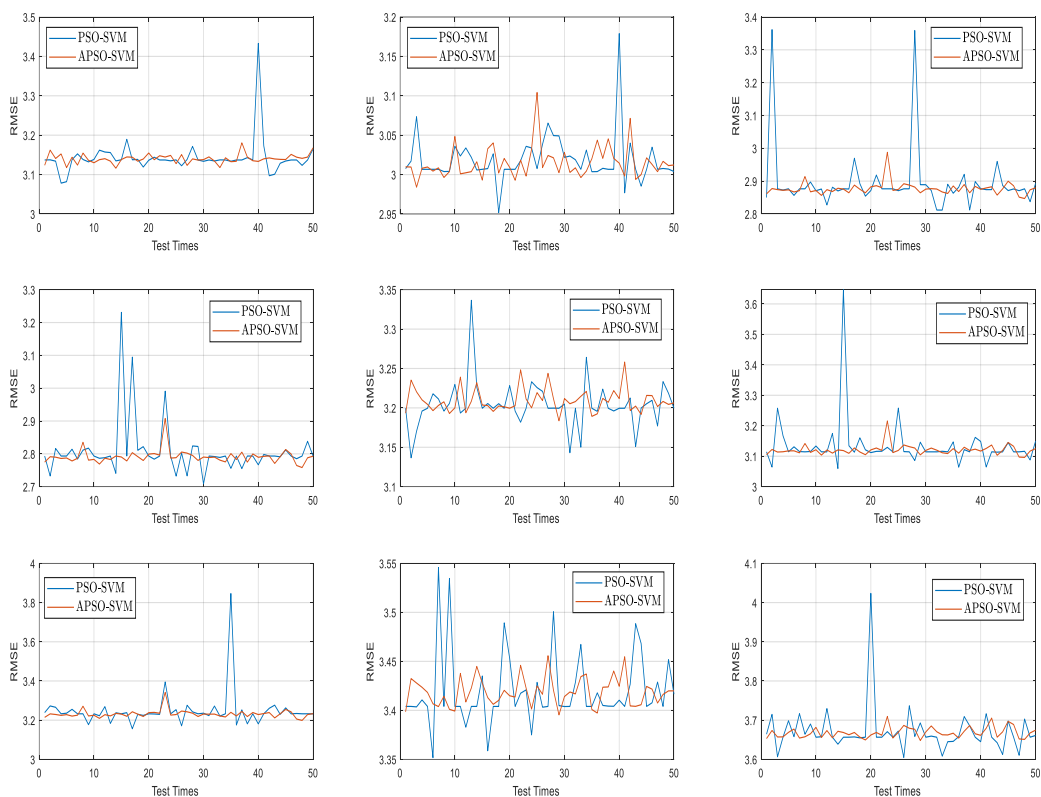


Figure 9. RMSE comparison of the two algorithms

As is shown in Figure 9, when the SOC discharge interval of the batteries is 100%-30%, the maximum error when PSO-SVM is used is 3.362, and the error when APSO-SVM is used is 2.9. At the same time, the SOH prediction diagram of battery #3 is made, which is shown in Figure 10. It is obvious that the prediction effect of battery #3 is significantly worse than that of battery #2, both of which have a certain error with the true value, which is also related to the slower decline of battery #3. There is a

certain difference in the distribution range of the test data and the training data, which causes the error to become larger.

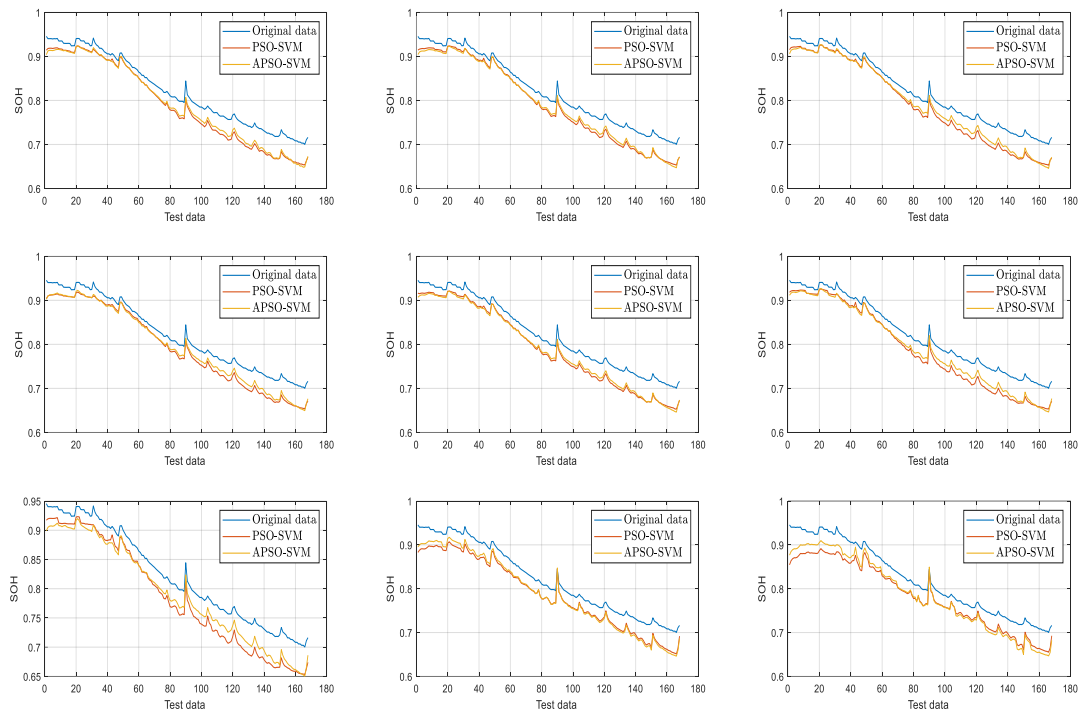
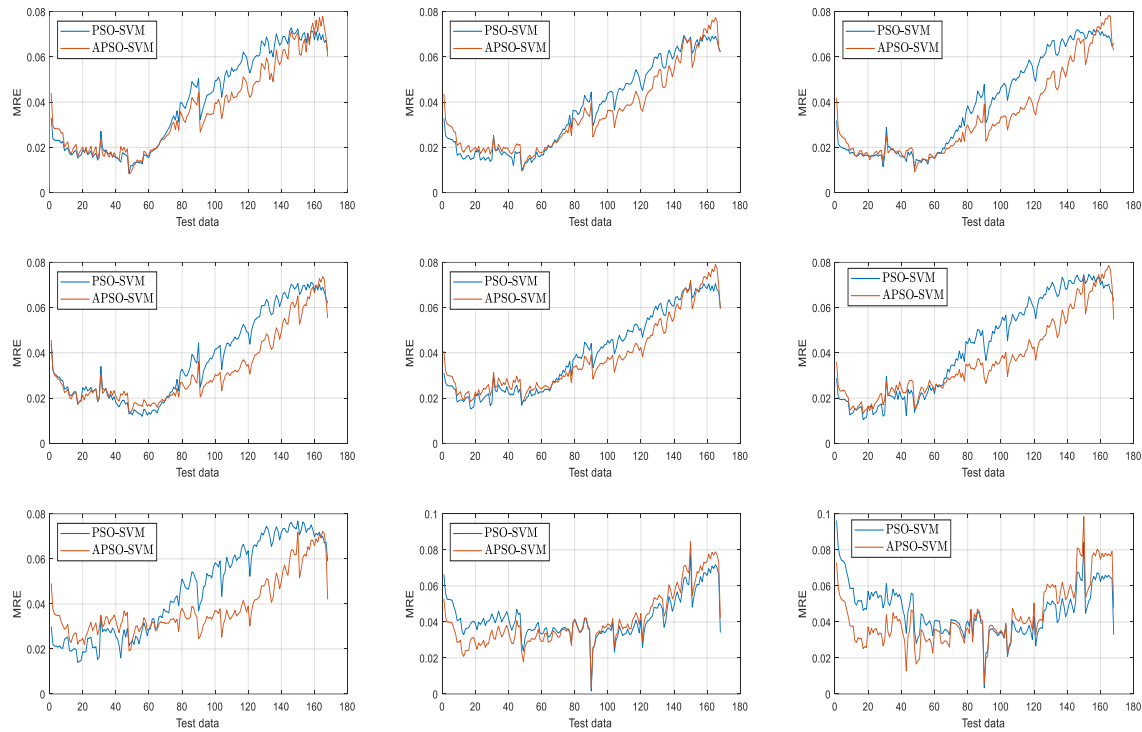


Figure 10. SOH prediction of battery #3

At the same time, a graph of estimated average relative error of battery #3 is made in this article. From the graph, it can be found that the average relative error when APSO-SVM is used is significantly lower than that of PSO-SVM, which shows that the use of APSO-SVM can improve the stability of estimation.

**Figure 11.** Comparison of mean relative error

5.3. Error comparative analysis

Khumprrom et al. [31] proposed a data-driven method to predict the SOH of batteries. The SOH estimation error of this method is 3.427. The estimation error is 2.61 when the PSO-SVM algorithm is used and 2.316 when the APSO-SVM algorithm proposed in this paper is used.

Table 2. Error comparison between different models

RMSE	k-NN	LR	SVM	ANN	DNN	PSO-SVM	APSO-SVM
	5.598	4.558	4.1831	4.611	3.427	2.610	2.316

It can be found that the accuracy of the PSO-SVM model integrated with AdaBoost has been improved. However, it should be noted that the main advantage of APSO-SVM is that a strong learner can be obtained by combining multiple weak learners, thus realizing risk diversification and reducing the probability of a single learner's estimation error at a certain moment.

6. CONCLUSION

The method of battery health estimation based on the AdaBoost-PSO-SVM algorithm proposed in this paper is a further research and expansion of the previous work [23].

First of all, the battery public data provided by NASA is used as simulation experimental data to extract the aging characteristics that affect the battery SOH. The SOH feature extraction described in the previous research work is not very vivid, and the color identification of 168 aging curves is not clear enough. Therefore, the color gradient method is used in this article to redraw the aging characteristic curve of the batteries. As the aging degree of the battery continues deepening, as shown in Figure 3 and 4, the color of the corresponding health status curve also changes from light blue to dark blue. As is shown in Figure 5, the color of the corresponding health curve changes from yellow to dark red. At the same time, the relationship between battery SOC and voltage is also supplemented in this article. As is shown in Figure 4, the dense part of the local curve is enlarged, and it is concluded that as the degree of aging continues deepening, the slope of SOC and discharge voltage gradually becomes smaller.

Secondly, establish a regression model of AdaBoost-PSO-SVM. The previous work has elaborated on how to realize the joint estimation of SOC and SOH. Therefore, this article will not elaborate on the estimation of SOC in detail, which is focused on the estimation stability of battery SOH instead. Multiple SVM sub-learners are used to train the training data, and the probability of an incorrect prediction is assigned to different SVM sub-learners according to certain weights, so as to achieve risk decentralization and avoid sudden PSO-SVM (single learner). Divergence leads to the problem of large estimation errors.

Then, the algorithm is used to test the test data, the APSO-SVM algorithm and the PSO-SVM algorithm are used to predict the SOH of 50 batteries, and a battery estimated RMSE chart is drawn, as is shown in Figure 6. It is not difficult to find that the PSO-SVM estimation will have large errors and is non-convergence. The overall estimation through APSO-SVM is relatively stable, which shows that the algorithm can be used to effectively improve the stability and accuracy of estimation. In addition, an adaptive analysis of the algorithm is also conducted in this article, a new battery is used to verify the effectiveness of the algorithm, and simulation analysis shows that the algorithm has a certain effectiveness.

Finally, relevant references for error comparative analysis are quoted in this article. The error of this algorithm is 2.316. Compared with the estimation errors of other algorithms, it shows that this algorithm can be used to improve the accuracy of estimation. Therefore, in summary, the method proposed in this paper based on the AdaBoost-PSO-SVM algorithm for health estimation of battery state can be used to effectively improve the stability and accuracy of battery SOH estimation, which has a certain adaptability and effectiveness.

CONFLICTS OF INTEREST

The authors declare there is no potential conflict of interest involved in this writing process.

ACKNOWLEDGMENTS

The Elite Project of Harbin University of Science and Technology under Grand LGYC2018JC026.

References

1. R. Li, S.H. Xu, S.B. Li, Y.Q. Zhou, K. Zhou, X.Z. Liu, J. Yao, *Ieee. Access*, 8(2020)10234-10242
2. K.S. Ng, C.S. Moo, Y.P. Chen, Y.C. Hsieh, *Appl. Energy*, 86(2009)1506-1511

3. H. Blanke, O. Bohlen, S. Buller, R.W. De Doncker, B. Fricke, A. Harnmouche, D. Linzen, M. Thele, D.U. Sauer, *J. Power. Sources*, 144 (2005) 418-425
4. Z.C. Xu, J. Wang, P.D. Lund, Y.M. Zhang, *Energy*, 225(2021)120160
5. T. D'Orazio, M. Leo, A. Distante, C. Guaragnella, V. Pianese, G. Cavaccini, *NDT&E. Int.*, 41(2007)145-154
6. S. Schwunk, N. Armbruster, S. Straub, J. Kehl, M. Vetter, *J. Power. Sources*, 239(2013)705-710
7. J. Bi, T. Zhang, H.Y. Yu, Y.Q. Kang, *Appl. Energ*, 182(2016)558-568
8. S. Jung, D. Kang, *J. Power. Sources*, 248(2014)498-509
9. G.K. Prasad, C.D. Rahn, *J. Power. Sources*, 232(2013)79-85
10. F. Luo, H.H. Huang, L.P. Ni, T. Li, *J. Energy. Storage*, 41(2021)102866
11. S. Cruz-Manzo, P. Greenwood, R. Chen, *J. Electrochem. Soc*, 164(2017)A1446-A1453
12. V. Klass, M. Behm, G. Lindbergh, *J. Power. Sources*, 270(2014)262-272
13. A. Nuhic, T. Terzimehic, T. Soczka-Guth, M. Buchholz, K. Dietmayer, *J. Power. Sources*, 239(2013)680-688
14. G.X. Bai, P.F. Wang, C. Hu, M. Pecht, *Appl. Energy*, 135(2014)247-260
15. X.N. Feng, C.H. Weng, X.M. He, X.B. Han, L.G. Lu, D.S. Ren, M.G. Ouyang, *Ieee. T. Veh. Technol.*, 68(2019)8583-8592
16. K.L. Liu, X.S. Hu, Z.B. Wei, Y. Li, Y. Jiang, *Ieee. T. Transp. Electr.*, 5(2019)1225-1236
17. H. Ji, W. Zhang, X.H. Pan, M. Hua, Y.H. Chung, C.M. Shu, L.J. Zhang, *Int. J. Energ. Res.*, 44(2020)6502-6510
18. L. Chen, Z.Q. Lu, W.L. Lin, J.Z. Li, H.H. Pan, *Measurement*, 116(2018)586-595
19. M.H. Hung, C.H. Lin, L.C. Lee, C.M. Wang, *J. Power. Sources*, 268(2014)861-873
20. E.R. Wogensen, B.R. Haverkort, M. Jongerden, R.R. Hansen, K.G. Larsen, 13th International Conference on Formal Modeling and Analysis of Timed Systems (FORMATS), Madrid, SPAIN, 2015, 305-320
21. J. Cannarella, C.B. Arnold, *J. Power. Sources*, 269(2014)7-14
22. Y.C. Zhang, C.Y. Wang, *J. Electrochem. Soc.*, 156(2009)A527-A535
23. R. Li, W.R. Li, H.N. Zhang, Y.Q. Zhou, W.L. Tian, *Front. Energy. Res.*, 9(2021)693249
24. Y. Freund, R.E. Schapire, *J. Comput. Syst. Sci*, 55(1997)119-139
25. Z.J. Cheng, Y.T. Zhang, C.H. Zhou, W.J. Zhang, S.B. Gao, *Int. J. Mol. Sci*, 10(2009)3316-3337
26. S.K. Wan, X.H. Li, Y.J. Yin, J. Hong, *Mech. Syst. Signal. Pr*, 156(2021)107671
27. F.F. Chen, M.T. Cheng, B.P. Tang, B.J. Chen, W.R. Xiao, *Meas. Sci. Technol*, 31(2020)105007
28. C. Ma, X. Zhai, Z.P. Wang, M.G. Tian, Q.S. Yu, L. Liu, H. Liu, H. Wang, X.B. Yang, *Int. J. Mach. Learn. Cyb*, 10(2019)2269-2282
29. M.S.H. Lipu, M.A. Hannan, A. Hussain, M.M. Hoque, P.J. Ker, M.H.M. Saad, A. Ayob, *J. Clean. Prod*, 205(2018)115-133
30. T.C. Qin, S.K. Zeng, J.B. G, *Microelectron. Reliab*, 55(2015)1280-1284
31. P. Khumprom, N. Yodo, *Energies*, 12(2019)660